General Disclaimer

One or more of the Following Statements may affect this Document

- This document has been reproduced from the best copy furnished by the organizational source. It is being released in the interest of making available as much information as possible.

- This document may contain data, which exceeds the sheet parameters. It was furnished in this condition by the organizational source and is the best copy available.

- This document may contain tone-on-tone or color graphs, charts and/or pictures, which have been reproduced in black and white.

- This document is paginated as submitted by the original source.

- Portions of this document are not fully legible due to the historical nature of some of the material. However, it is the best reproduction available from the original submission.
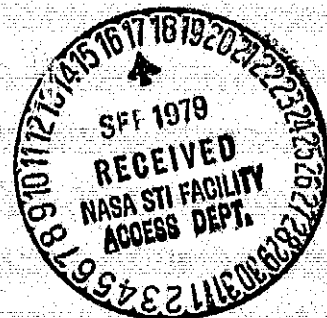
ANORTHITE: THERMAL EQUATION OF STATE

TO HIGH PRESSURES

by

Raymond Jeanloz

and

Thomas J. Ahrens

Seismological Laboratory
Division of Geological and Planetary Sciences
California Institute of Technology
Pasadena, California 91125

__Abstract:__

We present shock-wave (Hugoniot) data on single-crystal and porous anorthite ($CaAl_2Si_2O_8$) to pressures of 120 GPa. These data can be inverted to yield high pressure values of the Grüneisen parameter (γ), adiabatic bulk modulus (K_s) and coefficient of thermal expansion (α) over a broad range of pressures and temperatures which in turn are used to reduce the raw Hugoniot data and construct an experimentally-based, high-pressure thermal equation of state for anorthite. We find surprisingly high values of γ which decrease from about 2.2 to 1.2 over the density range 3.4 to 5.0 Mg/m^3. Our data clearly indicate that whereas the zeroth order anharmonic (quasi-harmonic) properties such as γ and α decrease upon compression for a single phase, these properties apparently increase dramatically (200% or more) in going from a low to a high pressure phase. The results for anorthite also support the hypothesis that higher-order anharmonic contributions to the thermal properties decrease more rapidly upon compression than the lowest order anharmonicities. We find an initial density $\rho_0 \sim 3.4$ Mg/m^3 for the "high-pressure phase" portion of the Hugoniot, with an initial value of K_s essentially identical to that of anorthite at zero pressure (90 GPa). This is surprising in light of recently documented candidate high-pressure assemblages for anorthite with significantly higher densities, and it raises the question of the nonequilibrium nature of Hugoniot data. By correcting the properties of anorthite to lower mantle conditions we find that although the density of anorthite is comparable to that of the lowermost mantle, its bulk modulus is considerably less, hence making enrichment in the mantle implausible except perhaps near its base.

Introduction

Anorthite is a mineral of particular geochemical interest because of
its refractory nature. Both theoretical and observational evidence suggest
that it is among the first, high temperature condensates that form from the
solar nebula and as such may be an important phase in the earliest accretional
history of the planets [e.g., Marvin, et al., 1970; Grossman and Larimer,
1974]. Indeed, according to inhomogeneous accretional models the present
internal zonation of the planets is thought to reflect, at least in a broad
sense, the accumulation of first the more refractory condensates followed by
successively more volatile-rich material [e.g., Turekian and Clark, 1969;
Clark, et al., 1972]. Hence anorthite and other calcium-aluminum minerals
may well be enriched deep within the earth and, if stable against buoyancy
forces, may remain there from the earliest times of the earth's formation. Recent
evidence has, in fact, suggested that a significant portion of the earth's
mantle could be quite enriched in a calcium component: the mineral CaO at
high pressures has properties which are virtually indistinguishable from those
of much of the lower mantle [Jeanloz, et al., 1979]. Except for the few
hundred kilometers near its base, however, the lower mantle appears to be
relatively homogeneous according to seismological observations, and the most
plausible location of a chemically distinct zone might be near the bottom of
the mantle [Anderson, 1975; Jeanloz and Richter, 1979].

The purpose of this paper is to present new high pressure data on
anorthite which provide among the most complete high-pressure, high-temperature
characterizations of any silicates to date. We have carried out shock-wave
experiments both on single-crystal anorthite and on anorthite containing a
substantial initial porosity. Because the states achieved in the latter

are much hotter than those produced in the nonporous (single-crystal) samples under shock, the temperature-dependence of the high-pressure equation of state can be directly evaluated. Thus, we derive a thermal equation of state for anorthite to pressures in excess of 120 GPa based on our data and with virtually no theoretical constraints on the form of such an equation of state. As a result, we have measurements over a wide range of pressures and temperatures of such thermal properties as the Grüneisen parameter and coefficient of thermal expansion, as well as the pressure- and temperature-dependent bulk modulus. This in turn allows us to make a direct comparison between anorthite at high pressures and the earth's interior, and leads us to the conclusion that although the density of anorthite is consistent with that of the lower mantle the bulk modulus probably precludes significant amounts of anorthite being present excent, possibly, in the lowermost portion of the mantle (D" region). A modest enrichment of anorthite is allowed by our data which would be stable at the base of the mantle, however none is required.

The porous anorthite used in our experiments is a lunar highlands rock (sample 60025). Its response to dynamic compression is of intrinsic interest for better understanding the cratering properties of the lunar surface. Because of its extremely primitive character, the properties of 60025 are of particular interest for modelling the late-stage accretion and early evolution of the moon. These considerations have been discussed more fully by Jeanloz and Ahrens [1978], in which some of the data which are described below were first presented.

Experimental

Euhedral, single-crystals of a "transitional" anorthite from Miyake-zima, Izu Islands, Japan [cf. Gay, 1954; Müller, et al., 1972; McLaren, 1973] were used as nonporous samples; their composition corresponds to $An_{95.4} Ab_{4.5} Or_{0.1}$ (representative analysis in Table 1). Samples were oriented morphologically for shock-wave propagation along the [010] direction and were prepared so as to avoid the small amounts of olivine ($Fo_{83}Fa_{17}$) inclusions present in the anorthite crystals. The porous anorthite samples were cut from lunar anorthosite 60025.36, .174 as previously described [Jeanloz and Ahrens, 1978].

The experimental techniques used in this study have been presented elsewhere and are only briefly discussed here [see Ahrens, et al., 1977; Jeanloz and Ahrens, 1977, 1978, 1979a]. The initial densities of samples are determined by an Archimedean and a bulk technique for nonporous and porous samples respectively. Properly characterizing the initial densities of the porous samples is particularly important for obtaining data of high quality [Jeanloz and Ahrens, 1978]. Shock experiments were carried out using a two-stage, light-gas gun or a 40 mm-bore, propellant gun to accelerate projectiles to velocities between 2.3 and 6.6 km/s. In each experiment, the impact velocity of the projectile is measured, as is the velocity of the shock wave which is generated in the sample upon impact by the projectile. The shock-wave velocity is determined by measuring the travel time of the shock-wave through the sample (of known thickness) by way of a rotating-mirror or an image-converter streak camera; details of the data reduction procedure are given in Jeanloz and Ahrens [1979a]. The Hugoniot state is then determined by applying impedance-matching conditions (Hugoniot equations) to the measured initial density, impact velocity and shock-wave velocity. A partially- or fully-released state is also determined by a free-surface or buffer impedance mismatch measurement,

reduced by way of the Riemann-integral formalism [e.g., Rice, et al., 1958; Lyzenga and Ahrens, 1978]. The standard equations of state of McQueen, et al., [1970] for W, Ta and 2024 Al alloy, and of Wackerle [1962] and Jackson and Ahrens [1979] for fused quartz were used in reducing these data.

Results

The results of the present experiments on single-crystal and porous anorthite are given in Tables 2 and 3, respectively, and are shown in Figures 1 and 2; for convenience, the data from Jeanloz and Ahrens [1978] for anorthosite 60025 are included, with slight corrections. Despite variations in composition and porosity, the present data can essentially be considered representative of endmember anorthite ($CaAl_2Si_2O_8$) with 0% and 19% initial porosity. Although the data of McQueen, et al., [1967] for Tahawus anorthosite correspond to a more sodic plagioclase (An_{49}), these are indistinguishable from the present (nonporous) data because the Tahawus anorthosite contains enough pyroxene to increase its initial density to that of anorthite (Figures 1 and 2). Hence the single-crystal anorthite and Tahawus anorthosite data are reduced together for determining the properties of anorthite at high pressures [see Jeanloz and Ahrens, 1978].

All of the present data are in the "high-pressure phase" regime [e.g., McQueen, et al., 1967] and for comparison a theoretical Hugoniot is shown in Figures 1 and 2 for the zero-pressure structure of anorthite. This is constructed [McQueen, et al., 1963; Davies and Gaffney, 1973] from a third-order Eulerian finite-strain adiabat, constrained by recent ultrasonic data for anorthite [Liebermann and Ringwood, 1976]. The Tahawus anorthosite data extrapolate to this theoretical Hugoniot at about 10.3 (±0.5) GPa pressure, indicating that the "mixed-phase" region extends from approximately 10.3 to 33.0

GPa for the non-porous samples. The porous and nonporous data in the "high-pressure phase" regime can be characterized by the least squares-fit, quadratic shock-wave velocity (U_s) versus particle velocity (u_p) relations given in Table 4 along with the average initial densities (ρ_0). Although the porous data require a quadratic U_s-u_p relation, this is not the case (statistically) for the nonporous data. It is interesting to note, however, that the porous and nonporous data define essentially parallel trends in Figure 2.

The release paths shown in Figure 1 are schematic in that they are constrained by only a single measurement in each case, as shown. In using the Riemann integral to derive these data, the release process is assumed to be isentropic, and hence the release paths are expected to have similar (but slightly smaller) slopes in the pressure-density plane as the Hugoniot. Although strictly isentropic release might seem implausible, Jeanloz and Ahrens [1979b] have recently shown that the effects of entropy production (excluding reactions or phase transformations) are not likely to be large enough to influence the release paths. The results for single-crystal anorthite and, at the higher pressures, porous anorthite are consistent with isentropic unloading. These release paths are significantly different from those documented in the "mixed-phase" region of feldspars in previous studies [Ahrens, et al., 1969b; Grady and Murri, 1976], consistent with the present data being in the "high-pressure phase" regime of the Hugoniot. It is difficult to understand, however, why several of the release paths for porous anorthite are steeper than the Hugoniot. Finite-strength effects appear not to be responsible and, although several possible explanations can be advanced, these results are enigmatic [cf. Jeanloz and Ahrens, 1978].

Thermal Properties

By combining shock-wave data from samples of different initial densities, thermal properties at high pressures can be derived with virtually no theoretical constraints involved [e.g., Kormer, et al., 1962; McQueen, et al., 1970; Jeanloz, 1979a]. In the following, thermal properties will be derived based on successively more extensive assumptions or approximations, however none of the results are strongly dependent on an assumed form of the high-temperature, high-pressure equation of state because each Hugoniot point represents a direct measurement of a pressure (P) - volume (V) - internal energy (E) state. The most important assumption is that the porous and nonporous data represent identical (or at least very similar) thermodynamic states, except for the temperatures involved; because of the large energies involved, this appears to be a good approximation [see Jeanloz, 1979a]. For example, despite the fact that the porous Hugoniot probably represents molten anorthite to a large extent, the effect of melting on density at a riven (high) pressure is   small: at zero pressure, a volume change on melting of only 4% is found [Skinner, 1966], and at high pressures this undoubtedly decreases to within the few percent accuracy of the Hugoniot data. Hence the effect of melting on the energies or compressibilities involved are not likely to be resolvable, and no anomalies which could be ascribed to melting are seen among the data considered here. Each datum probably represent an average over a heterogeneous thermal state achieved on the Hugoniot, particularly for the porous anorthite in which extremely high temperatures can be achieved along grain boundaries [e.g., Belyakov, et al., 1974, 1977; also, Grady, 1977]. However, for the hydrostatic condition which is (at least approximately) achieved along the Hugoniot, temperature perturbations result in density (rather than

pressure) variations. Thus, temperature variations between 10^4 and 10^5 K, and concentrated within about 10% of the sample, could readily be concealed within the 1-2% accuracy to which Hugoniot densities were determined in this study. At these high temperatures other processes, such as radiative thermal conductivity, are likely to become important enough to preclude more extreme temperature variations. The reproducibility of the present data also suggest that an adequate thermal average has been measured.

The porous and nonporous data are directly inverted to yield values of the Grüneisen parameter ($\gamma \equiv V \left(\frac{\partial P}{\partial E} \right)_V$) based on the Hugoniots given in Table 4. At a given volume (V_H) the Grüneisen parameter is given by

$$\gamma(V_H) = V_H \frac{2 \, (P_H^P - P_H^N)}{P_H^P \, (V_0^N - V_H) - P_H^N \, (V_0^P - V_H)}, \tag{1}$$

where 0 and H subscripts represent zero-pressure and Hugoniot states, while P and N indices refer to porous and nonporous samples respectively (further details are given in Jeanloz [1979a]) Equation 1 yields values of γ which are averaged over large temperature intervals and it is assumed here, as is commonly done [e.g., McQueen, et al., 1970; Wallace, 1972], that γ is essentially independent of temperature. Independent analyses show this to commonly be the case [e.g., Anderson, et al, 1968; Jeanloz, 1979a], and the porous data for anorthite, although available within only a small variation of initial porosities, are also consistent with a temperature-independent Grüneisen parameter.

The resulting values of γ are shown in Figure 3 in which each datum point represents the offset of a porous Hugoniot point from the nonporous Hugoniot. The error bars largely reflect uncertainties in the nonporous Hugoniot which must be extrapolated downward considerably in pressure (or density) for this

analysis. Because the porous Hugoniot is quite well constrained by our data, a smooth $\gamma(\rho)$ curve can be derived from the parameters listed in Table 4 (Figure 3) which compares favorable with a power-law fit to the data

$$\gamma = 2.20 \ (3.40V)^{1.66(\pm 0.42)} \tag{2}$$

with V in m^3/Mg (based on $\rho_0 = 3.40$ Mg/m^3: see below). It is interesting to note that the exponent in Equation 2 is   larger than 1, as in the case of iron [Jeanloz, 1979a], although a value of unity is often assumed for the volume dependence of the Grüneisen parameter (e.g., McQueen, et al., 1967, 1970; Brennan and Stacey, 1979].

The most striking feature in Figure 3 is the dramatic increase in γ from its zero-pressure value, for the high density states achieved along the anorthite Hugoniot. The Grüneisen parameter is expected to decrease upon compression (as shown by the present data), hence the increase shown in Figure 3 at $\rho < 3.7$ Mg/m^3 directly reflects the large increase in zeroth-order anharmonic (quasi-harmonic) contributions to the thermal properties of anorthite as it is compressed through the "mixed-phase" region. It may seem surprising that anharmonic properties increase across such a density jump, however this effect is seen in other cases, such as the phase transitions in Fe, Bi and halides [Jeanloz, 1979a; Ramakrishnan, et al., 1979]. This is consistent with the standard interpretation of the "mixed-phase" region of the Hugoniot [e.g., McQueen, et al., 1967] as representing a polymorphic transformation to a high-density, high-pressure phase, perhaps with increased cation-coordination number. In general, an increase in coordination number is accompanied by an increase in average bond length and hence an increase in anharmonicity might be expected. However, other effects are also available

to explain the observed increase in γ with density, such as slight changes

in the nature of the interatomic bonding [e.g., Megaw, 1938]. In any case,

an increase in anharmonic contributions to the thermodynamic properties of

anorthite when shock-compressed into its high-density state is clearly

indicated by the present data.

Given a knowledge of the Grüneisen parameter, an isentropic bulk modulus

(K_s) or bulk sound speed (c) can be determined from the slope of the Hugoniot

at any given density (or pressure) by means of the following equation

[e.g., Al'tshuler, et al., 1960; McQueen, et al., 1967, 1970]

$$\rho_H c_H^2 = K_s\Big)_H = \left(\frac{dP_H}{dV_H}\right)\left[\left(V_0^P - V_H\right)\frac{\gamma}{2V_H} - 1\right]V_H + \frac{1}{2}P_H^N \gamma \quad . \qquad [3]$$

This equation is derived by assuming a Mie-Grüneisen form for the equation of

state, however the thermal correction to the Hugoniot slope is small and is

experimentally constrained (through γ), therefore minimizing the effect of

this assumption. The resulting values of K_s along the Hugoniot of anorthite

are shown in Figure 4. Again, the individual points are determined by the

offset of the porous anorthite data while the curves for K_s along the porous

and nonporous Hugoniots are determined from the parameters given in Table 4

[cf. Jeanloz, 1979a]. The error bars on the data mainly reflect uncertainties

in the fit to the nonporous Hugoniot, particularly of its slope. Significantly,

both the porous and nonporous Hugoniots are well enough constrained to directly

yield independent measurements of the bulk modulus of anorthite at high pressures

and at widely varying temperatures (corresponding to different initial porosity).

However, in order to quantitatively separate the thermal and compressional

effects on the bulk modulus, a more complete model must be derived for anorthite

under shock conditions, as is done below. Such a model yields estimates of the

temperatures along the porous and nonporous Hugoniots, thus allowing the
isotherms shown in Figure 4 to be determined.

Sound velocities have been independently measured in (alkali) feldspars
under shock by means of unloading waves [Grady, et al., 1975]. These
velocities were considered to be anomalously low, and hence were interpreted
as being bulk (rather than longitudinal) velocities, suggesting the possibility
of partial melting during shock loading. The present results, however, yield
lower bulk sound speeds along the Hugoniot than were expected by Grady and
coworkers, thus obviating the need to invoke their "shear-band" melting.
In fact, a direct comparison of their velocities with the present data allows
the shear modulus along the Hugoniot of feldspar to be calculated. This
yields $\mu \sim 117.3$ and 118.3 GPA (Poisson's ratio of 0.21-0.26) at pressures of
34.5 and 46.0 GPa respectively, assuming that Grady, et al. measured longitudinal
velocities. These values for the shear modulus are not unreasonable, but they
are only approximate since there are significant uncertainties in the data
sets which are being compared and compositional differences between the samples
are ignored. In any case, this analysis suggests that nonporous feldspar melts
along the Hugoniot at pressures significantly higher than 46 GPa. Similar
comparisons of unloading wave velocities with independently determined bulk
compressibility have been used to determine the shear properties of metals
to pressures well in excess of 100 GPa [e.g., Al'tshuler, et al., 1971; Simonov
and Chekin, 1975].

Anorthite behaves as though it undergoes a major phase transformation
under shock, as exemplified by the large density increase and anomalously
high (apparent) compressibility through the "mixed-phase" region. Without
specifying the details of such a transformation, the important consequence is
that the properties of anorthite along the "high-pressure phase" branch of the

Hugoniot must be referenced to a zero-pressure density which is significantly higher than the initial density of anorthite and that the densification through the "mixed-phase" region is reflected not as a thermal energy but as a potential energy which is imparted to the (static) lattice: that is, an energy of transformation (ΔE_{tr}). By comparing the theoretical (untransformed) Hugoniot with the nonporous Hugoniot of anorthite at about 30 (± 10) GPa pressure, a volume decrease of about 20% is found associated with the "mixed-phase" region. Hence, the high-pressure anorthite data correspond to a state with a zero-pressure density ρ_{02} = 3.40 (± 0.1) Mg/m^3, a Grüneisen parameter given by Equation 2 and with $\Delta E_{tr} \sim 198 \pm 60$ kJ/mol. Here, $\Delta S_{tr} \sim 0$ was assumed and the transition pressure of 10.3 GPa derived above was used.

With these parameters constrained, a principal adiabat can immediately be derived for the porous and nonporous anorthite data corresponding to the "high-pressure phase" branch of the Hugoniot. The approach used here was to find a least-squares fit to the data with the adiabat given by either third - or fourth-order, Eulerian finite-strain theory. The appropriate equations for the forward problem [e.g., McQueen, et al., 1963; Davies, 1973] are readily converted to normal equations of the form:

$$\frac{2}{3} \left\{ \left[1 - \frac{\gamma}{2}\left(\frac{\rho_H}{\rho_{01}} - 1\right) \right] P_H + \gamma\rho_H \Delta E_{tr} \right\} \left\{ x^3 (x^2-1) \zeta \right\}^{-1} = \beta_0 + \beta_1$$

$$(x^2-1) \left[\frac{\gamma}{2} (x^2-1) - x^2\right] \zeta^{-1} \qquad [4]$$

with

$$\zeta = \chi^2 - \frac{3}{4} \gamma (\chi^2-1) + \xi_2 (\chi^2-1)^2 [\chi^2 - \frac{3}{8} \gamma (\chi^2-1)] \qquad [5a]$$

$$\xi_2 = \frac{3}{8} K_{02}K_{02}'' + \frac{3}{8} K_0' (K_0' - 7) + \frac{143}{24} \qquad [5b]$$

$$\chi = (\rho/\rho_{02})^{1/3} \qquad [5c]$$

The least-squares solution to Equation 4 yields best estimates of the parameters $\beta_0 = K_{02}$ and $\beta_1 = K_{02}\xi_1$, where $\xi_1 = \frac{3}{4} (4 - K_{02}')$ and all properties refer to the adiabat centered at ρ_{02} (primes indicate pressure derivatives). Although Equation 4 can easily be extended to the multivariate case in which ξ_2 and ΔE_{tr} could be independently estimated, these variables are so poorly constrained by a fit to the data (at least in the present case) that no further information is gained. A third-order fit (corresponding to a Birch-Murnaghan adiabat) is derived by setting $\xi_2 = 0$ in Equation (5a), resulting in

$$K_{0s} = 86.5 \ (\pm 10) \ GPa \qquad [6a]$$

$$K_{0s}' = 3.93 \ (\pm 0.20) \qquad [6b]$$

$$K_{0s}K_{0s}'' = -3.45 \ (\pm 0.35) \qquad [6c]$$

for the adiabat corresponding to the "high-pressure phase" Hugoniot of anorthite; the value in Equation 6c comes from Equation 5b. Alternatively, fourth-order solutions can be found for Equation 4, however these do not improve the fit to the data significantly and do not change the resulting adiabat markedly.

For example, letting $K_{0s}'' = 0$ ($\xi_2 = 1.49$) yields $K_{0s} = 95.4$ GPa, $K_{0s}' = 2.93$ and an adiabat which is within about 0.7% in density from that determined by Equation 6. It is interesting that K_0' is essentially equal to 4 (Equation 6b), the value for the Birch, second order equation of state, whereas neither the Slater, Dugdale-MacDonald nor Free Volume estimates of γ based on this value agree with the present data [e.g. Zarkov and Kalinin, 1971].

The bulk modulus given in Equation 6a is surprisingly low given the large increase in density from $\rho_{01} = 2.74$ Mg/m^3 to $\rho_{02} = 3.4$ Mg/m^3 (compare with $K_{0s} = 92$ GPa for anorthite at zero pressure: Liebermann and Ringwood [1976]), however this conclusion is in complete agreement with the results originally derived by McQueen et al., [1967]. Because the Grüneisen parameter was not independently known in that earlier study, they derived solutions for the principal adiabat of the "high-pressure phase" Hugoniot of anorthosite using both low ($\gamma_0 = 1.13$) and high ($\gamma_0 = 1.73$) values of γ (they assumed $\gamma/V =$ constant). The values of γ measured in the present study clearly favor the latter solution, which resulted in $\rho_{02} = 3.46$ Mg/m^3, $K_{0s} = 88$ GPa and $K_{0s}' = 3.93$, in excellent agreement with the values found here despite the different formalism used to reduce the Hugoniot data. Ironically, subsequent work in which the seismic equation of state of Anderson [1967, 1969] was assumed to hold [Anderson and Kanamori, 1968; Ahrens et al., 1969a; Davies and Anderson, 1971] had tended to favor the low-γ solution of McQueen and coworkers ($\rho_{02} = 3.53$ Mg/m^3, $K_{0s} = 112$ GPa), resulting in values of ρ_{02} between 3.57 and 3.71 Mg/m^3. In the present study, no solution could be found using Equations 2 and 4 which fit the data and which was consistent with either form of the seismic equation of state [Anderson, 1967. 1969]; it is worth noting that the seismic parameter and density of anorthite are not consistent with the seismic equation of state at zero pressure.

The present results (using Equations 6) are shown in Figure 5, along with the nonporous and porous Hugoniots directly determined by the data. A metastable Hugoniot for anorthite (centered on ρ_{02} = 3.4 Mg/m^3) can be derived by rearranging Equation 4, with $\rho_{01} = \rho_{02}$ and ΔE_{tr} = 0. It is shown in Figure 5 along with a Hugoniot calculated for 10% initially porous anorthite which is derived from Equations 1 and 2, as can be done for Hugoniots corresponding to arbitrary porosities. The bulk moduli along the adiabat, metastable Hugoniot and calculated, porous Hugoniot(s) then follow directly from the theory of finite strains [Birch, 1938, 1947; Davies, 1973] or, for the Hugoniots, from Equation 3; the results are displayed in Figure 4 (the calculated, porous Hugoniot results are left off for clarity).

In order to derive the temperatures along the compression curves shown in Figure 5, a model for the specific heat at constant volume (C_v) must be constructed, except for the case of the adiabat along which the temperature is completely determined by the Grüneisen parameter:

$$T_s(\rho) = T_{0s} \exp \frac{\gamma_0 - \gamma}{n} , \qquad [7]$$

where $\gamma(\rho)$ is given by Equation 2; γ_0 = 2.20, n = 1.66, and T_{0s} = 300K. The temperature along any compression curve (e.g., a Hugoniot) can be calculated from:

$$T(P,\rho) = T_s(\rho) + \int_{P_s}^{P} \frac{V\,dP'}{\gamma\,C_v} ; \qquad [8]$$

subscript s indicates evaluated along the principal adiabat and P' is a dummy variable. In order to solve Equation 8, a simple, Debye-Grüneisen model is

used to evaluate the specific heat, as has commonly been done in previous studies [e.g., Ahrens, et al., 1969b; McQueen, et al., 1970]. A (high-temperature) value of the Debye temperature $\theta_1 \sim 1000K$ was found from the zero-pressure specific heat data of anorthite [Robie, et al., 1978], however this must be renormalized to the high-pressure state centered at $\rho_{02} = 3.4$ Mg/m^3. According to Debye theory, the characteristic temperature is proportional to both a mean sound velocity and density, however because the mean velocity of the high-pressure state is unknown (and velocity systematics apparently do not satisfy the data) the following relation was used [see Anderson, et al., 1968, for example]:

$$\theta_2 \sim \theta_1 \, (\rho_{02}/\rho_{01})^{1/3} = 1075 \text{ K}. \qquad [9]$$

In Equation 9, the mean velocity is assumed constant in going to the high-pressure state and only the density jump is accounted for. This is a rough approximation, but the approximations used here mainly affect the computed results at temperatures less than θ: about 1100 to 2200K for pressures up to 120 GPa. Note that the Debye temperature depends on volume according to a relation analogous to Equation 7. Because the temperature along the adiabat is given independently, only the temperature along the metastable Hugoniot below about 80 GPa is likely to be seriously affected either by the use of the Debye-Grüneisen model or by the choice of θ_2. We note that higher than zeroth order anharmonic contributions to the specific heat, such as the linear - T term [e.g., Wallace, 1972], are ignored although they may alter the specific heat somewhat at high temperatures. The overall effect is not likely to be very significant, however, particularly because the higher order anharmonicity

is expected to decrease rapidly upon compression [Zharkov and Kalinin, 1971].

The temperatures calculated in this fashion are shown in Figure 6. The largest uncertainties arise from uncertainties in ΔE_{tr}, followed by uncertainties in the principal adiabat of Figure 5. This might be expected since a change in ΔE_{tr} from 200 to 300 kJ/mol involves a temperature change $\delta T \backsim \delta E / C_v \backsim \frac{100}{0.32} \backsim 300K$ at a given density, and ΔE_{tr} is not very well constrained.

The calculated temperatures also allow isotherms to be found for the high-temperature, high-pressure bulk modulus data in Figure 4. Given the uncertainties and extrapolations involved these isotherms must be considered somewhat shcematic, but it is interesting to note the change in pressure derivative of the bulk modulus with temperature and also the relative insensitivity of the bulk modulus to temperature at high pressures and moderately low temperatures. For example at 100 GPa, $\left| \left(\frac{\partial K_S}{\partial T} \right)_P \right|$ apparently increases from about 6×10^{-3} GPa K^{-1} at 4000K to about 30×10^{-3} GPa K^{-1} at 7000K, a value typical of the region of broadly spaced isotherms between the porous and nonporous Hugoniot curves in Figure 4. This range of values is also compatible with the low pressure data summarized by Anderson et al., [1968].

The coefficient of thermal expansion is given by

$$\alpha = \gamma C_v \ (VK_s - \gamma^2 TC_v)^{-1} = \frac{\gamma C_p}{V \ K_s} \qquad [8]$$

in which the specific heat at constant pressure (C_p) is distinguished from C_v. Equation 8 can be solved as a function of pressure and temperature from the present results on anorthite, as shown in Figure 7 in which both isobars and isochores are displayed. For comparison, the zero-pressure data for anorthite and the high-pressure Debye temperature are also shown. At temperatures below θ,

the values of α in Figure 7 are subject to errors due to the possible inadequacies of the specific heat model used. However the thermal expansion must vanish as the temperature goes to zero and the general features of Figure 7 are not strongly model-dependent.

Although the zero-pressure thermal expansion of anorthite is subject to some uncertainty, it is significantly lower than the low-pressure thermal expansions derived from the "high pressure phase" Hugoniot data (Figure 7). As with the Grüneisen parameter, the thermal expansion of anorthite increases considerably upon compression to the high-pressure state ($\rho_0 = 3.40$ Mg/m^3), whence it decreases with increasing pressure. Again, this can be viewed in terms of anharmonic effects increasing sharply at a pressure-induced phase transformation, whereas pressure decreases both γ and α for a given phase. This decrease of thermal expansion with compression can be approximately related to the bulk modulus isotherms in Figure 4 since $\left(\dfrac{\partial \alpha}{\partial P}\right)_T = K_T^{-2}\left(\dfrac{\partial K_T}{\partial T}\right)_P \sim K_s^{-2}\left(\dfrac{\partial K_s}{\partial T}\right)_P$ (K_T is the isothermal bulk modulus).

At high temperatures (T>Θ) α increases with temperature, particularly at low pressures. This is due to both zeroth and first-order anharmonic effects which are approximately of equal importance in increasing α: the former through $C_p = (1+\alpha\gamma T)C_v$, while the latter derive from the decrease in the bulk modulus with temperature. It is important to note that these anharmonic contributions decrease more rapidly with pressure than does the ze.oth order effect embodied in the thermal expansion itself. Hence at pressures above 80–100 GPa, α attains a "saturated", high-temperature value above the Debye temperature. In this "saturated" regime, the calculated values of the thermal expansion are virtually model-independent since the Dulong-Petit value of C_v provides a good approximation for C_p and all other variables in Equation 8 are experimentally constrained [cf. Jeanloz, 1979a]. Furthermore, the relative decrease in importance of

higher-order anharmonic contributions relative to the lower-order (e.g. strictly quasiharmonic) effects provides additional justification for the simple. Debye-Grüneisen model which was used for C_v. From the present data, the second Grüneisen parameter [e.g., Anderson, et al., 1968] $\delta_s = \alpha K_s \left(\frac{\partial K_s}{\partial T}\right)_p$ appears to be relatively independent of temperature at high pressures and temperatures, as expected. Unfortunately, δ_s is not very well constrained ($\delta_s \sim 2.2 \pm 1.2$), however it can be evaluated over many tens of GPa and thousands of degrees, and its approximate constancy lends further support to the assumed temperature independence of γ[Anderson, et al., 1968].

Discussion

Much of the preceding analysis depends on the inference that anorthite undergoes, in some sense, a phase transformation under shock-loading to pressures above about 10.3 GPa. Although previous analyses have assumed this to be the case [e.g., McQueen, et al., 1967; Anderson and Kanamori, 1968; Ahrens, et al., 1969a; Davies and Anderson, 1971], there is considerable doubt that polymorphic transformation occurs under shock in a fashion directly analogous to the phase transformations achieved under static conditions. Because of kinetic limitations, it is quite likely that highly nonequilibrium states are measured in these shock experiments.

One indication of such idfficulties arises from a comparison of the present reduction of the Hugoniot data on anorthite in the "high-pressure phase" regime with the densities of predicted high-pressure phases or assemblages given in Table 5. As shown in Figure 5, the zero-pressure densities of these candidate high-pressure phases are considerably higher than is found from the reduced hugoniot data. Although neither the hollandite phase nor the mixed-oxide assemblage have been documented for anorthite, both the calcium ferrite- and

sodium titanate-bearing assemblages have been synthesized in calcium-aluminum-silicate systems [Reid and Ringwood, 1969; Liu, 1978b] and Liu [1978a] has found Na-plagioclase in the hollandite structure. Previous reductions of the Hugoniot data had allowed higher zero-pressure densities than are found here. However, the new data on the Grüneisen parameter preclude such solutions and, as discussed above, the use of the seismic equation of state in those studies appears to be unwarranted. Regardless of other assumptions, no solutions could be found to Equations 2, 4 and 5 which fit the data with ρ_{02} larger than about 3.80 ($\pm$0.10) Mg/m^3. In fact, the best fits to the present data resulted from allowing ρ_{02} < 3.0 Mg/m^3 and ΔE_{tr} = 0, however yielding seemingly unphysical values of K_{0s} (typically less than 50 GPa). These results suggests that anorthite along the Hugoniot is not transformed to an equilibrium high-pressure polymorph, particularly since less than 30 GPa pressure has been required to find the assemblages listed in Table 5. A recent study of Jeanloz [1979b] finds little evidence for the transformation of (nonporous) silicates in Hugoniot experiments either from observations on shocked olivine samples or from theoretical consider-ations, and anorthite may provide the first clear case of a silicate achieving significantly more efficient packing under static as compared to dynamic loading.

On the other hand, it is not certain that the results of static high-pressure experiments can be so directly compared with the shock-wave data since the temperatures achieved in the former ($\sim$1000-1500K) are for the most part considerably less than the temperatures achieved along the Hugoniot. More important, though, is the fact that strict equilibrium on a microstructural state need not be required for the kind of analysis presented here. As illustrated above for the case of melting, large energy differences are involved in this analysis such that rather substantial deviations from equilibrium values are not likely to be noted in the Hugoniot data. Furthermore, the evidence for a density

increase of about 20% above 10 GPa, as well as the release adiabats of non-porous anorthite, are all indicative of the behavior of a high-pressure phase. As discussed by Jeanloz [1979b], despite the Hugoniot possibly not representing equilibrium states, the properties measured under shock appear to be very close to their equilibrium values.

There are two problems which must be specifically addressed in this context. Although values of total energy are reasonably well constrained in this analysis, the partitioning of energy may not be. In particular, the amount of thermal energy present, and hence the calculated temperatures, depend on the estimate value of ΔE_{tr}: if anorthite undergoes no manner of phase transformation under shock $\Delta E_{tr} = 0$. Jeanloz [1979b] used this fact and measured Hugoniot temperatures to argue that some form of (nonequilibrium) transformation apparently occurs in silicates under shock. Similarly, if melting occurs in the anorthite samples this would no affect the bulk thermal or compressional properties severly, but it could change the calculated temperatures dramatically, lowering them (at a given pressure) by possibly 10^3K. Since the zero-pressure melting temperature of anorthite is 1830K, a simple scaling argument suggests that melting may occur at about 70-90 GPa on the nonporous Hugoniot or about 40-60 GPa along the porous Hugoniot. This ambiguity can, however, be directly resolved by way of shock-temperature measurements or by determinations of the shear modulus along the Hugoniot. Higher order effects associated with melting, such as discussed by Grover [1971], are not likely to change the values of properties calculated here by more than 15-20% even at the highest temperatures shown in Figure 6; given the important decrease in higher-order anharmonicities with pressure this is likely to be an overly conservative estimate.

The second question is whether the phase(s) along the "high-pressure phase" Hugoniot evolve continuously with increasing pressure, as might particularly be expected if these are in highly nonequilibrium states. This is equivalent to considering all of the data presented here as being in a "mixed-phase" regime despite the break in the U_s-u_p relation documented in Figure 2 [cf. McQueen, et al., 1967, for example]. Some question has, in fact, been raised for other silicates [Jeanloz and Ahrens, 1977; Jackson and Ahrens, 1979] about stability in the "high-pressure phase" regime: some evidence suggests continued reaction or evolution along the Hugoniot to pressures of 100 GPa or higher. Although the measured Hugoniot densities might still be used in such a case, the reduction of the Hugoniot data and especially the values of bulk moduli derived above would be meaningless. At present there is no compelling evidence for such a conclusion and counterexamples can be found, however the inability to independently verify this is problematical. Hence, just as the porous and nonporous Hugoniots are assumed to be directly comparable, the "high-pressure phase" branch of the Hugoniot is assumed to represent a single (possibly nonequilibrium) phase or assemblage.

Lower Mantle

Since theories involving inhomogeneous accretion of the planets suggest that relatively refractory compounds, such as anorthite, may exist deep within the earth, it is of interest to compare the present data with seismologically-based models of the lower mantle. In Figures 4 and 5 the density and bulk modulus of the mantle are compared with our data for anorthite. The density of anorthite is compatible with mantle densities, but only for pressures in excess of about 80 to 100 GPa. As is evident from Figure 4, however, the bulk moduli derived here for anorthite at high pressures virtually preclude its being

a major component throughout the bulk of the lower mantle [cf. McQueen et al., 1967]. If the assumptions made in calculating the bulk moduli are in error, then higher (more compatible) values would be found for anorthite.

Whereas a recent study on CaO [Jeanloz et al., 1979] indicates that the lower mantle could be considerably enriched in calcium, the present data do not support anorthite as being a particularly important Ca-bearing mineral in the mantle except possibly in its lowermost portions (D'' region). Because the D'' region is seismologically anomalous it is not possible to determine its properties, with great confidence. Indeed, the evidence for a decrease in velocity gradient through the D'' region (see the review of Cleary [1974], for example) is compatible with its containing 10-20% anorthite (or similar refractory compound) according to the present data, while for plausible mantle temperatures [e.g., Stacey, 1977; Jeanloz and Richter, 1979] anorthite has a density within about 1% of the observed mantle densities at this level. Although not required, an enrichment of anorthite in the D'' region is therefore acceptable and would appear to be bouyantly stable. This is consistent with a simple thermal model for the lower mantle presented by Jeanloz and Richter [1979], in which the D'' region is chemically distinct from the overlying mantle. An increase in refractory components toward the base of the mantle is also in qualitative agreement with inhomogeneous accretion models, however a simple zone-refining process could produce the same effect in an originally homogeneous mantle heated from below.

Conclusions

New shock-wave data have been presented for anorthite from which a full
high-temperature, high-pressure equation of state has been derived. Whereas
anorthite has relatively low values of thermal expansion and Grüneisen
parameter at zero pressure, these attain relatively high values in the high
density state corresponding to the "high-pressure phase" Hugoniot, but
decrease upon compression as expected. Higher order anharmonic contributions
appear to decrease more rapidly with pressure and the thermal expansion
therefore saturates to a high temperature value at pressures above about
100 GPa. Reduction of the Hugoniot data allows shock temperatures to be
calculated and also yields a principal adiabat for the high pressure branch of
the Hugoniot. This adiabat has an initial bulk modulus (about 87 GPa) which is
essentially identical to that of anorthite, whereas the initial density is
about 3.40 Mg/m^3. Because candidate, high-pressure assemblages with
significantly higher densities are known for anorthite (4.05 to 4.30 Mg/m^3)
and because Hugoniot states are not likely to be at equilibrium, an ambiguity
arises in the interpretation of the present data which are assumed to reflect
equilibrium properties. Nevertheless, this assumption appears to be valid and
no inconsistencies are evident. Significantly, no solutions could be found in
reducing the data with zero-pressure densities for the principal adiabat above
3.8-3.9 Mg/m^3, or with bulk moduli satisfying the seismic equation of state.
A reduction of these data to lower mantle conditions demonstrate that anorthite
may be present in amounts of 10-20% in the D'' region, but it is not likely to be a
significant phase elsewhere in the lower mantle because of its apparently small
bulk modulus.

References

Ahrens, T. J., D. L. Anderson and A. E. Ringwood (1969a). Equations of state and crystal structures of high-pressure phases of shocked silicates and oxides. Rev. Geophys., 7, 667-707.

Ahrens, T. J., C. F. Petersen and J. T. Rosenberg (1969b). Shock compression of feldspars, J. Geophys. Res., 79, 2727-2746.

Ahrens, T. J., I. Jackson and R. Jeanloz (1977). Shock compression and adiabatic release of a titaniferous mare-basalt. Proc. Lunar Sci. Conf. 8th, 3437-3455.

Al'tshuler, L. V., M. I. Brazhnik and G. S. Telegin (1971). Strength and elasticity of iron and copper at high shock-wave compression pressures. J. Appl. Mec. Tech. Phys., 12, 921-926.

Al'tshuler, L. V., S. B. Kormer, M. I. Brazhnik, L. A. Vladimirov, M. P. Speranskaya and A. I. Funtikov (1960). The isentropic compressibility of aluminum, copper, lead and iron at high pressures, Sov. Phys. JETP, 11, 766-775.

Anderson, D. L. (1967). A seismic equation of state, Geophys. J. R. astr. Soc., 13, 9-30.

Anderson, D. L. (1969). Bulk modulus-density systematics, J. Geophys. Res., 74, 3857-3864.

Anderson, D. L. (1975). Chemical plumes in the mantle. Bull. Geol. Soc. Am., 86, 1593-1600.

Anderson, D. L. and R. S. Hart, (1976). An earth model based on free oscillations and body waves. J. Geophys. Res., 81, 1461-1475.

Anderson, D. L. and H. Kanamori (1968). Shock-wave equations of state for rocks and minerals. J. Geophys. Res., 73, 6477-6502.

Anderson, O. L., E. Schreiber, R. C. Liebermann and N. Soga (1968).

Some elastic constant data on minerals relevant to geophysics. Rev.

Geophys., 6, 491-524.

Anderson, S. and A. D. Wadsley (1961). The crystal structure of $Na_2Ti_3O_7$.

Acta Cryst., 14, 1245-1249.

Belyakov, G. V., L. D. Livshits and V. N. Rodionov (1974). Shock-wave

deformation of an inhomogeneous medium which is modelled by a set of

steel balls. Izv. Earth Phys., no. 10, 665-667.

Belyakov, G. V., V. N. Rodionov and V. P. Samosadnyi (1977). Heating of

porous material under impact compression. Combustion, Explosion and

Shock Waves, 13, 524-528.

Birch, F. (1938). The effect of pressure upon the elastic parameters of

isotropic solids, according to Murnaghan's theory of finite strain.

J. App. Phys., 9, 279-288.

Birch, F. (1947). Finite elastic strain of cubic crystals. Phys. Rev., 71,

809-824.

Brennan, B. J. and F. D. Stacey (1979). A thermodynamically based equation

of state for the lower mantle. J. Geophys. Res., in press.

Clark, S. P., K. K. Turekian and L. Grossman (1972). Chemical models of the

Earth, in: The Nature of the Solid Earth (E. C. Robertson, ed.),

McGraw-Hill, New York, pp. 3-18.

Cleary, J. R. (1974). The D'' region. Phys. Earth Planet. Int., 9, 13-27.

Davies, G. F. (1973). Quasi-harmonic finite strain equations of state of

solids. J. Phys. Chem. Solids, 34, 1417-1429.

Davies, G. F. and D. L. Anderson (1971). Revised shock-wave equations of

state for high-pressure phases of rocks and minerals. J. Geophys. Res.,

76, 2617-2627.

Davies, G. F. and E. S. Gaffney (1973). Identification of high-pressure phases of rocks and minerals from Hugoniot data. Geophys. J. R. astr. Soc., 33, 165-183.

Dziewonski, A. M., A. L. Hales and E. R. Lapwoo' (1975). Parametrically simple earth models consistent with geophy: :al data. Phys. Earth Planet. Int., 10, 12-48.

Gay, P. (1954). The structure of the plagioclase feldspars. V. Min. Mag., 30, 428-438.

Grady, D. E. (1977). Processes occurring in shock wave compression of rocks and minerals, in: High-Pressure Research (M. H. Manghnani and S. Akimoto, eds.) Academic Press, New York, pp. 389-438.

Grady, D. E. and W. J. Murri (1976). Dynamic unloading in shock compressed feldspar. Geophys. Res. Lett., 3, 472-474.

Grady, D. E., W. J. Murri and P. S. DeCarli (1975). Hugoniot sound velocities and phase transformations in two silicates. J. Geophys. Res., 80, 4857-4861.

Grossman, L., J. W. Larimer (1974). Early chemical history of the solar system. Rev. Geophys. Space Phys., 12, 71-101.

Grover, R. (1971). Liquid metal equation of state based on scaling. J. Chem. Phys., 55, 3435-3441.

Jackson, I. and T. J. Ahrens (1979). Shock-wave compression of single-crystal forsterite. J. Geophys. Res., in press.

Jeanloz, R. (1979a). Properties of iron at high pressures and the state of the core. J. Geophys. Res., 84.

Jeanloz, R. (1979b). Shock effects in olivine and implications for Hugoniot data. J. Geophys. Res., submitted.

Jeanloz, R. and T. J. Ahrens (1977). Pyroxenes and olivines: structural implications of shock-wave data for high pressure phases, in: High-Pressure Research (M. H. Manghnani and S. Akimoto, eds.) Academic Press, New York, pp. 439-461.

Jeanloz, R. and T. J. Ahrens (1978). The equation of state of a lunar anorthosite: 60025, Proc. Lunar Planet. Sci. Conf. 9th, 2789-2803.

Jeanloz, R. and T. J. Ahrens (1979a). FeO and CaO: Hugoniot equations of state of two oxides,

Jeanloz, R. and T. J. Ahrens (1979b). Release adiabat measurements on minerals: the effect of viscosity, J. Geophys. Res., submitted.

Jeanloz, R., T. J. Ahrens, H. K. Mao and P. M. Bell (1979). B1/B2 transition in CaO from shock-wave and diamond cell experiments. Science (in press)

Jeanloz, R. and F. M. Richter (1979). Convection, composition and the thermal state of the lower mantle. J. Geophys. Res., in press.

Kormer, S. B., A. I. Funtikov, V. D. Urlin and A. N. Kolesnikova (1962). Dynamic compression of porous metals and the equation of state with variable specific heat at high temperatures. Sov. Phys. JETP, 15, 477-488.

Liebermann, R. C. and A. E. Ringwood (1976). Elastic properties of anorthite and the nature of the lunar crust. Earth Planet. Sci. Lett., 31, 69-79.

Liu, L.-G. (1978a). High-pressure phase transformations of albite, jadeite and nepheline. Earth Planet. Sci. Lettr., 37, 438-444.

Liu, L.-G. (1978b). A new high-pressure phase of $Ca_2Al_2SiO_7$ and implications for the earth's interior. Earth Planet. Sci. Lett., 40, 401-406.

Lyzenga, G. and T. J. Ahrens (1978). The relations between the shock-induced free-surface velocity and post-shock density of solids. J. App. Phys., 49, 201-204.

Marvin, U. B., J. A. Wood and J. S. Dickey, Jr. (1970). Ca-Al rich phases in the Allende meteorite. Earth Planet. Sci. Lett., 7, 346-350.

McLaren, A. C. (1973). The domain structure of a transitional anorthite: a study by direct lattice-resolution electron microscopy. Contrib. Mineral. Petrol., 41, 47-52.

McQueen, R. G., J. N. Fritz and S. P. Marsh (1963). On the equation of state of stishovite. J. Geophys. Res., 68, 2319-2322.

McQueen, R. G., S. P. Marsh and J. N. Fritz (1967). Hugoniot equation of state of twelve rocks. J. Geophys. Res., 72, 4999-5036.

McQueen, R. G., S. P. Marsh, J. W. Taylor, J. N. Fritz and W. J. Carter (1970). The equation of state of solids from shock wave studies, in: High Velocity Impact Phenomena (R. Kinslow, ed) Academic Press, New York, pp. 294-419 and Appendices.

Megaw, H. D. (1938). The thermal expansion of crystals in relation to their structure. Z. Kristallog., 100, 58-76.

Müller, W. F., H. R. Wenk and G. Thomas (1972). Structural variations in anorthite. Contrib. Mineral. Petrol., 34, 304-314.

Ramakrishnan, J., R. J. Hardy and G. C. Kennedy (1979). The Grüneisen parameter γ of KBr, RbCl and Bi through high pressure phase transitions. J. Phys. Chem. Solids, 40, 297-303.

Reid, A. F. and A. E. Ringwood (1969). Newly observed high pressure transformations in Mn_3O_4, $CaAl_2O_4$ and $Zr SiO_4$. Earth Planet. Sci. Lett., 6, 205-208.

Rice, M. H., R. G. McQueen and J. M. Walsh (1958). Compressibility of solids by strong shock waves, Solid State Physics, 6, 1-63.

Ringwood, A. E. (1975). Composition and Petrology of the Earth's Mantle, McGraw-Hill, New York, 618 pp.

Robie, R. A., B. S. Hemingway and J. R. Fisher (1978). _Thermodynamic Properties of Minerals and Related Substances_ U.S. Geol. Survey Bull. 1452 Washington, D.C., 456 pp.

Simonov, I. V. and B. S. Chekin (1975). High-velocity collisions of iron plates. _Combustion, Explosion and Shock Waves_, 11, 237-242.

Skinner, B. J. (1966). Thermal expansion, in: _Handbook of Physical Constants_ (S. P. Clark, Jr., ed.) _Geol. Soc. Am. Mem. 97_, pp. 75-96.

Stacey, F. D. (1977). A thermal model of the earth. _Phys. Earth Planet. Int._, 15, 341-348.

Touloukian, Y. S., R. K. Kirby, R. E. Taylor and T. Y. R. Lee (1977). _Thermal Expansion, Nonmetallic Solids_, IFI/Plenum, New York, 1658 pp.

Turekian, K. K. and S. P. Clark, Jr. (1969). Inhomogeneous accretion model of the earth from the primitive solar nebula. _Earth Planet. Sci. Lett._, 6, 346-348.

Wackerle, J. (1962). Shock-wave compression of quartz. _J. App. Phys._, 33, 922-937.

Wallace, D. C. (1972). _Thermodynamics of Crystals_, J. Wiley & Sons, New York, 484 pp.

Walsh, J. M. and R. H. Christian (1955). Equation of state of metals from shock wave measurements. _Phys. Rev._, 97, 1544-1556.

Zharkov, V. N. and V. A. Kalinin (1971). _Equations of State for Solids at High Pressures and Temperatures_, Consultants Bureau, New York, 257 pp.

TABLE 1

Electron Microprobe Analysis

Single-Crystal Anorthite (Miyake-zima, JAPAN)

Oxide	Weight %
Na_2O	0.51
MgO	0.04
Al_2O_3	35.28
SiO_2	44.19
K_2O	0.02
CaO	19.57
FeO	0.66
TOTAL	100.27

TiO_2, BaO, Cr_2O_3, MnO, F, Cl absent

TABLE 2

SINGLE-CRYSTAL ANORTHITE [1] HUGONIOT DATA

Experiment			Sample Initial Density	Hugoniot State				Release State[2]			
Shot No.	Flyer/ Driver	Impact Velocity (km/s)	Crystal (Mg/m³)	Shock wave Velocity (km/s)	Particle Velocity (km/s)	Pressure (GPa)	Density (Mg/m³)	Shock-wave velocity (km/s)	Particle Velocity (km/s)	Pressure (GPa)	Density (Mg/m³)
LGG 058	2024 Al	5.398 ±0.005	2.783 ±0.002	7.400 ±0.077	2.911 ±0.012	60.0 ±0.4	4.588 ±0.043	6.226 ±0.119	3.226 ±0.075	44.3 ±1.9	4.459 ±0.088
LGG 038	Ta	4.925 ±0.003	2.756 ±0.001	8.628 ±0.057	3.791 ±0.005	90.2 ± 0.5	4.916 ±0.030	7.932 ±0.079	4.333 ±0.050	76.2 ±1.6	4.455 ±0.127
LGG 037	Ta	5.694 ±0.004	2.768 ±0.002	9.477 ±0.092	4.338 ±0.009	113.8 ± 0.9	5.104 ±0.050	8.722 ±0.181	4.798 ±0.113	92.2 ±4.1	4.861 ±0.164

NOTES: (1) [010] shock-wave propagation direction

(2) Derived from measured shock-wave velocity (U_s) through fused quartz buffer-mirror using $U_s = 1.108 + 1.587\, u_p$, $\rho_0 = 2.204$ Mg/m³

TABLE 3

LUNAR ANORTHOSITE (60025) HUGONIOT DATA

Experiment			Sample		Hugoniot State				Release State			
			Initial Density									
Shot No.	Flyer/ Driver	Impact Velocity (km/s)	Bulk (Mg/m³)	Crystal(1) (Mg/m³)	Shock-wave Velocity (km/s)	Particle Velocity (km/s)	Pressure (GPa)	Density (Mg/m³)	Shock-wave Velocity (km/s)	Particle Velocity (km/s)	Particle(2) Pressure (GPa)	Density (Mg/m³)
40mm Gun												
429	W	2.312 ±0.010	2.243 ±0.014	2.747 ±0.002	5.070 ±0.021	2.036 ±0.010	23.2 ± 0.2	3.749 ±0.025	Free Surface Velocity: 3.727 ±0.101		0	2.563 ±0.091
LGG												
042	2024Al	4.971 ±0.002	2.239 ±0.010	2.751 ±0.003	6.751 ±0.038	2.964 ±0.009	44.8 ± 0.2	3.990 ±0.025	5.523 ±0.036	2.783 ±0.023	33.9 ± 0.5	3.943 ±0.025
LGG 029	Ta	4.467 ±0.006	2.244 ±0.002	2.709 ±0.003	7.732 ±0.048	3.617 ±0.005	62.7 ± 0.3	4.216 ±0.027	6.434 ±0.109	3.355 ±0.069	47.5 ± 1.8	4.137 ±0.039
LGG 059	Ta	5.240 ±0.020	2.216 ±0.002	2.767 ±0.005	8.539 ±0.046	4.211 ±0.017	79.7 ± 0.05	4.372 ±0.032	8.031 ±0.110	4.363 ±0.059	77.2 ± 2.3	4.199 ±0.314
LGG 036	Ta	5.668 ±0.003	2.199 ±0.001	2.743 ±0.006	9.150 ±0.072	4.525 ±0.006	91.1 ± 0.6	4.351 ±0.939	8.116 ±0.086	4.417 ±0.054	79.0 ± 1.8	4.333 ±0.039
LGG 026	Ta	5.762 ±0.012	2.234 ±0.003	2.713 ±0.002	9.168 ±0.129	4.591 ±0.015	94.0 ± 1.1	4.473 ±0.075	6.952 ±0.255	3.682 ±0.164	56.4 ± 4.6	4.074 ±0.096
LGG 061	Ta (thin)	6.585 ±0.005	2.230 ±0.024	2.748 ±0.006	10.142 ±0.121	5.176 ±0.019	117.5 ± 1.5	4.573 ±0.075	9.349 ±0.207	5.194 ±0.130	107.0 ± 5.1	4.573 ±0.075

Notes: (1) Archimedean density: assumes interconnected porosity. Average crystal density is 2.74 Mg/m³ and the average porosity is about 19%.

(2) Derived from measured shock-wave velocity through fused quartz buffer-mirror using $U_s = 1.108 + 1.587 u_p$, $\rho_0 = 2.204$ Mg/m³.

TABLE 4

ANORTHITE: HUGONIOT EQUATIONS OF STATE

Non-porous

$\rho_o = 2.74 \ (\pm 0.02) \ \text{Mg/m}^3 \ , \ P > 30 \ \text{GPa}$

$U_s = 2.37 \ (\pm 0.55) + 1.82 \ (\pm 0.36) \ u_p - 0.045 \ (\pm 0.058) \ u_p^2$

Porous

$\rho_o = 2.23 \ (\pm 0.03) \ \text{Mg/m}^3 \ , \ P > 22 \ \text{GPa}$

$U_s = 1.43 \ (\pm 0.35) + 1.90 \ (\pm 0.20) \ u_p - 0.044 \ (\pm 0.028) \ u_p^2$

TABLE 5

CANDIDATE HIGH-PRESSURE PHASES

FOR ANORTHITE $(CaAl_2Si_2O_8)$

Hollandite phase: $^{VIII}Ca\ ^{VI}(Al_2Si_2)O_8$, $\rho_o = 3.92$ Mg/m^3 (based on Liu, 1978a)

Mixed Oxides assemblage: $^{VI}AcO + ^{VI}Al_2O_3 + 2\ ^{VI}SiO_2$, $\rho_o = 3.95$

OR

$^{VIII}CaO + ^{VI}Al_2O_3 + 2\ ^{VI}SiO_2$, $\rho_o = 4.05$ Mg/m^3

(CaO data from Jeanloz, et al., 1979)

Calcium Ferrite assemblage: $^{VIII}Ca\ ^{VI}Al_2O_4 + 2\ ^{VI}SiO_2$, $\rho_o = 4.10$ Mg/m^3

(Reid and Ringwood, 1969)

Sodium Titanate assemblage: $\frac{1}{2}\ ^{VIII}Ca\ ^{VI}Al_2\ ^{VI}SiO_7 + ^{VI}Al_2O_3 + 3\ ^{VI}SiO_2$,

$\rho_o = 4.29$ Mg/m^3 (Liu, 1978b; Anderson and Wadsley, 1961)

General References: Ringwood (1975), Robie, et al., (1978)

Figure Captions

Figure 1: Anorthite and anorthosite shock-wave data from the present study and that of McQueen, et al., [1967] compared with a theoretical Hugoniot for anorthite (its uncertainty corresponds to variations in the assumed pressure derivative of the bulk modulus between 4 and 6). The porous and nonporous Hugoniot curves are from the fit listed in Table 4.

Figure 2: The data and Hugoniot curves from Figure 1 shown in the shock-wave velocity vs. particle velocity plane. The dashed line corresponds to the theoretical Hugoniot of (untransformed) anorthite, while c_0 shows the bulk sound speed of anorthite from Liebermann and Ringwood [1976].

Figure 3: Grüneisen parameter of anorthite as a function of density. The present data at densities above 3.5 Mg/m^3 are shown as individual points which can be fit by a power law in density with an exponent of 1.66 (Equation 2). Alternatively, the best-fit Hugoniots of Table 4 imply values of the Grüneisen parameter which are given by the short-dashed curve. The zero-pressure value for anorthite is shown at a density of 2.74 Mg/m^3 along with an assumed volume dependence (long dashes). Data sources: Liebermann and Ringwood [1976]; Rigby and Green, and Floyd in Touloukian, et al., [1977]; Robie, et al., [1978].

Figure 4: Adiabatic bulk modulus of anorthite as a function of pressure
and temperature based on the present shock-wave data, compared
with seismological values for the lower mantle [Dziewonski,
et al., 1975; Anderson and Hart, 1976]. Bulk moduli based
directly on data are shown for the (nonporous) Hugoniot and
proous Hugoniot, along with values along the adiabat and
metastable Hugoniot derived from the reduced Hugoniot data.
Isotherms based on the calculated temperatures are also given
(thin, solid lines), with temperatures given in K.

Figure 5: Hugoniots given by the data on anorthite (heavy lines) are
compared with the derived compression curves based on the
present reduction of the shock-wave data (thin lines). The
density in the lower mantle according to Dziewonski et al. [1975]
and Anderson and Hart [1976] is presented (dashed lines), as
the zero-pressure densities of candidate high-pressure
assemblages corrsponding to anorhtite (see Table 5).

Figure 6: Calculated temperatures along the porous (19%) and nonporous
Hugoniot of anorthite, as well as the derived adiabat and
metastable Hugoniot. Estimated errors are shown for the
Hugoniot temperatures.

Figure 7: Coefficient of thermal expansion of anorthite as a function of
pressure and temperature. Isobars (heavy curves) and density
isopleths (thin, dashed curves; densities in Mg/m^3 in parentheses)
are shown for the high-pressure state of anorthite. The Debye
temperature (Θ) used in this analysis is also given, as a function
of density (or pressure). Along each isobar, the circles correspond
to intersections with, respectively, the adiabat (open), metastable
Hugoniot (open), Hugoniot (filled) and porous Hugoniot (filled)
with increasing temperature. For comparison, the thermal expansion
of anorthite measured at zero-pressure is shown with a dotted curve
extending to the melting temperature (marked) according to a fit
to the data of Rigby and Green, and Floyd in Touloukian, et al.,
[1977], and also as crosses from the work of Kozu et al., [in
Skinner, 1966].

ANORTHITE

Legend:
- HUGONIOT STATE } THIS STUDY
- RELEASED STATE }
- ○ ANORTHOSITE, TAHAWUS (McQueen, et al)

NON-POROUS HUGONIOT

POROUS HUGONIOT

THEORETICAL HUGONIOT (UNTRANSFORMED)

NON-POROUS SAMPLES

POROUS SAMPLES

POROUS SAMPLES

DENSITY (Mg/m^3)

PRESSURE (GPa)

ANORTHITE

— THIS STUDY
○ ANORTHOSITE, TAHAWUS (McQueen, et. al)

PARTICLE VELOCITY (km/s)

SHOCK-WAVE VELOCITY (km/s)

POROUS HUGONIOT

NON-POROUS HUGONIOT

C_0

ANORTHITE

n=1.66

$U_S - u_p$ fit

γ/V constant

GRÜNEISEN PARAMETER

DENSITY (Mg/m³)

ANORTHITE

PRESSURE (GPa)

TEMPERATURE (K)

POROUS HUGONIOT

HUGONIOT

METASTABLE HUGONIOT

ADIABAT